Modeling and Simulation of a Biomimetic Underwater Vehicle

Chris Watts

Dept of Electronics & Electrical Engineering
University of Glasgow
Rankine Building
Oakfield Avenue
G12 8LT
c.watts@elec.gla.ac.uk

Euan McGookin

Dept of Aerospace Engineering
University of Glasgow
James Watt Building
G12 8QQ
e.mcgookin@eng.gla.ac.uk

Keywords: Biomimetic, robot fish, underwater vehicle

Abstract
This paper describes work carried out at the University of Glasgow investigating biomimetic fish-like propulsion systems for underwater vehicles. The development of a simple mathematical model is described for a biomimetic fish like vehicle which utilizes a tendon drive propulsion system. This model is then compared with a model of a vehicle of similar size but with a propeller for main propulsion. Simulation results for both models are shown and compared.

1. INTRODUCTION

The past few decades have seen a dramatic increase in the interest in Autonomous Underwater Vehicles (AUVs) from various fields such as the oil industry, military and oceanographic research for numerous applications [Wernli, R.L., 2002].

In recent years there has been a growing interest in applying biomimetic concepts to underwater vehicles with many projects investigating fish-like propulsion [Yu, Junzhi, et al, 2005], [Liu, J et al 2005]. It has been suggested that there are potential benefits that may be obtained from using fish like propulsion over conventional propeller based propulsion such as improved propulsion system efficiency [Triantafyllou, M.S., Triantafyllou, G.S., 1995], increased maneuverability [Wolfgang, et al, 1999] and decrease disturbance of surrounding water [Sfakiotakis, M., et al, 1999]

There are a number of potential applications that vehicles utilizing a biomimetic propulsion system may be particularly suited to due to the properties of their propulsion system. Such applications include environmental monitoring, where the presence of conventional vehicle with a propeller may disturb the surroundings; certain military applications where the use of a tail may provide a degree of stealth over a noisy propeller.

1.1 RoboSalmon Project

RoboSalmon is the name given to the low cost prototype vehicles under development for this project at the University of Glasgow. As the name implies these biologically inspired robotic vehicles are based on the anatomy of Atlantic Salmon [Young, J.Z., 1962].

The reason for imitating an Atlantic Salmon is due to the interesting lifecycle of this fish. Each salmon is spawned in a river, then as it matures it migrates to sea and eventually returns to the same river to reproduce and die [Young, J.Z., 1962].

One of the aims of the project is to investigate different methods for actuating the fish-tail propulsion system based on simulation models. These models enable each system to be evaluated in terms of swimming performance and overall efficiency. Thus the models of the propulsion systems are used as the design specifications for the vehicles. Another aspect of the project is to compare the biomimetic RoboSalmon vehicles to a vehicle of similar size but with a conventional propeller/rudder combination for propulsion/maneuvering.

Currently only one RoboSalmon has been constructed, shown in Figure 1, which utilizes a tendon drive actuation scheme, and limited testing carried out.

Figure 1. 1st RoboSalmon Prototype

The remainder of this paper is organized as follows. Section 2 gives an overview of the development of the mathematical model of the tendon drive RoboSalmon vehicle. Section 3 describes a model of a vehicle of similar size and shape to the Robosalmon but utilizing a propeller and rudder for main propulsion. Section 4 presents some simulation results for the vehicles described in Sections 2 and 3. Finally, Section 5 discusses the conclusions that can be drawn from the work so far and outlines the next stage of the project.

2. ROBOSALMON MODEL

A significant part of this project is the development of mathematical models of the RoboSalmon vehicles. The aim of developing simple models of the vehicles is to allow for the performance of the systems to be estimated before construction of the hardware and for the development of appropriate control systems to deploy on the hardware. The first model to be developed is the RoboSalmon which utilizes a tendon drive actuation system for the biomimetic propulsion system. Using the model framework also allows different DC motors to be evaluated in terms of their effectiveness in the propulsion systems.

The tendon drive system uses two parallel tendon wires which run the length of the tail with one end of the tendons fixed to the caudal fin assembly and the other attached to the arms of a servo motor. The tail is comprised of ten revolute joints with a rigid fin attached to the tenth joint. As the servo motor arm rotates it pulls on one of the tendons which causes the revolute joints to turn and produces the effect of the tail bending. The rotational reciprocal motion of the servo arm thus produces a flapping motion similar to that of a fish tail. It is thought that using this system for propulsion and maneuvering may provide some benefits as only one motor is required, whereas in conventional systems one motor would be required for the propeller and another would be needed to actuate the rudder.

The model developed for the tendon drive RoboSalmon consists of three main parts – the propulsion system modeling, vehicle dynamics and vehicle kinematics.

2.1 Propulsion System Modeling

The aim of modeling the propulsion system is to allow for estimates of the thrust and maneuvering forces to be made using the input commands to the system. For the model the system has been subdivided into four sections as shown in Figure 2.

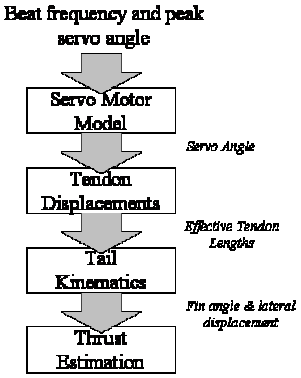

Figure 2. Tendon Drive Propulsion system flowchart

2.1.1 Servo Motor Model

For actuation of the tendon drive system a Hitec HS-5645 Digital Servo [Hitec RCD, 2007] motor is used. This servo operates by moving the output servo arm to an angular position which corresponds to the pulse width of the input pulse width modulated (PWM) signal.

This servo motor system is modeled as a DC motor with a reduction gearbox attached. The standard electrical and mechanical equations for a DC motor [Franklin, G.,et al, 1991], which are shown in Equations (1) and (2), are used to describe the motor.

$$L\frac{di}{dt} + Ri = V - K_e\dot{\theta} \quad (1)$$

$$J\ddot{\theta} + b\dot{\theta} = K_t i - T_l \quad (2)$$

Where L is the inductance of the motor (Henrys), I is the motor current (Amps), R is the motor resistance (Ohms), V is the applied voltage (Volts), K_e is the motor emf constant ($Vrad^{-1}s^{-1}$), θ is the motor angular displacement (radians), J is the inertia of the motor shaft and load (kgm^2), b is the viscous friction coefficient, K_t is the motor torque constant (NmA^{-1}) and T_l is the load torque (Nm).

It is assumed that a PID controller is used within the servo for positional control of the servo arm [Behnke, S., Schreiber, M., 2006].

Commands are sent to this servo which generates a rotational reciprocal motion of between ±45 degrees. The maximum frequency of this motion is limited to approximately 1Hz due to the mechanical limitations of the whole tendon drive system.

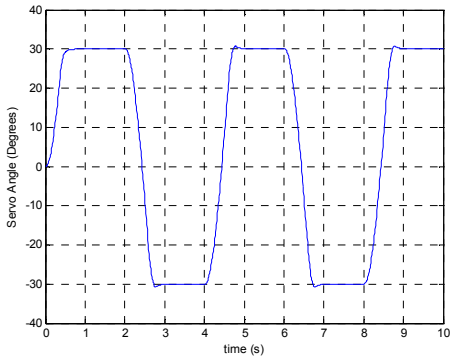

Figure 3. Simulated servo response to step changes of ±30degrees

Figure 3 shows the simulated servo motor response to a step commands for ±30degrees. This indicates that the servo motor model is able to represent the motions required by the tendon drive application with adequate response time.

2.1.2 Tendon Displacements

The effective displacement of the tendons due to the motion of the servo arm is calculated by applying basic trigonometry to the geometry of the system layout. A more detailed description can be found in [Watts, C., et al 2007].

2.1.3 Tail Kinematics

The mechanical tendon drive tail is modeled as ten revolute joints with a rigid fin attached to the last revolute joint. By using the representation it allows for the system to be modeled in a similar fashion to a robot manipulator. As such the kinematic equations used to describe robot manipulators can be applied to describe the tendon drive tail [Craig, J., 1989. The standard method used to model the forward kinematics of robot manipulators is the Denavit-Hartenberg (D-H) representation [Niku, S.B., 2001]. This method involves assigning each joint a reference frame according to a set procedure as shown in Figure 4.

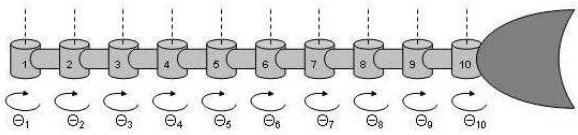

Figure 4. D-H Representation of tail with 10 revolute joints

Using this representation allows for determination of the lateral displacement of the caudal fin with reference to the first joint frame attached to the body using the joint variables (θ_1 to θ_{10}) for the variable revolute joints.

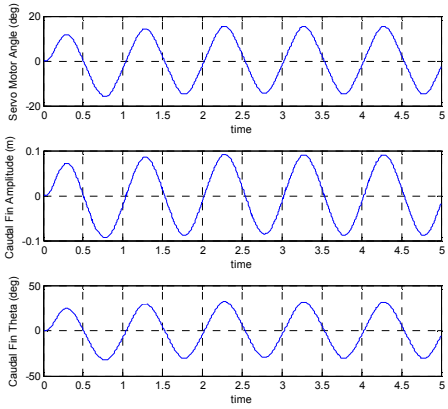

Figure 5. Simulate tendon drive system kinematics.

The graphs presented in Figure 5 show the servo motor arm angular position (top), the caudal fin tip amplitude (middle) and the caudal fin tip angular displacement. The last two calculated tail variables are used to estimate the thrust produced by the tail, as described below.

2.1.4 Thrust Estimation

Using the tail motions calculated in the previous sections the thrust produced by the tail movements is estimated using a derivation of Lighthill's Large Amplitude Elongated Body Theory [Lighthill, M.J., 1960] shown in [Wardle, C.S., Reid, A., 1975].

To carry out simple turning maneuvers the centerline of the tail oscillations are altered. The thrust force produced by the tail acts along this altered centerline and the thrust components lateral and perpendicular to the vehicle hull are used to generate a yawing moment and a sway force. This is illustrated in Figure 6.

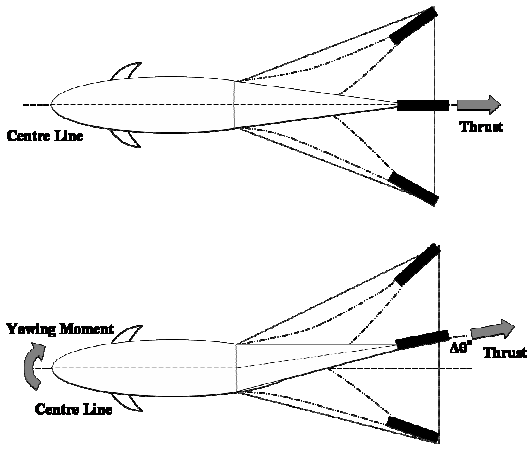

Figure 6. Diagram of thrust force when tail beat centered (top) and offset (bottom)

2.2 Vehicle Dynamics

The dynamics of the RoboSalmon vehicle in 6 degrees of freedom are modeled using the standard equation for modeling marine craft [Fossen, T.I., 1994] shown in Equation (3).

$$\boldsymbol{M}\dot{\upsilon}+\boldsymbol{C}(\upsilon)\upsilon+\boldsymbol{D}(\upsilon)\upsilon+\boldsymbol{g}(\eta)=\tau \qquad (3)$$

where $\boldsymbol{M}$ is the added mass and inertia matrix, $\boldsymbol{C}$ is the Corolois terms, $\boldsymbol{D}$ is the damping matrix, $\boldsymbol{g}(\eta)$ is the gravitational and buoyancy terms, τ is the input forces and moments generated by the tail and $\boldsymbol{\upsilon}$ is the velocity vector as shown in equation 4.

$$\upsilon=\begin{bmatrix}u & v & w & p & q & r\end{bmatrix}' \qquad (4)$$

A number of simplifying assumptions are made in relation to the modeling of the dynamics of the vehicle. The vehicle hull is assumed to be a prolate ellipsoid in shape. The vehicle is also assumed to be neutrally buoyancy although in practice this is difficult to achieve [Burcher, R. and Rydill, L., 1994].

Terms for the added mass effects due to operation in a water environment are included in the Mass and Corolis matrices [Fossen, T.I., 1994] and are shown in Equations (5) and (6).

$$M=\begin{bmatrix} m-X_{\dot{u}} & 0 & 0 & 0 & 0 & 0 \\ 0 & m-Y_{\dot{v}} & 0 & 0 & 0 & 0 \\ 0 & 0 & m-Z_{\dot{w}} & 0 & 0 & 0 \\ 0 & 0 & 0 & J_x-K_{\dot{p}} & 0 & 0 \\ 0 & 0 & 0 & 0 & J_y-M_{\dot{q}} & 0 \\ 0 & 0 & 0 & 0 & 0 & J_z-N_{\dot{r}} \end{bmatrix} \qquad (5)$$

$$C=\begin{bmatrix} 0 & 0 & 0 & 0 & w(m-Z_{\dot{w}}) & v(Y_{\dot{v}}-m) \\ 0 & 0 & 0 & w(Z_{\dot{w}}-m) & 0 & u(m-X_{\dot{u}}) \\ 0 & 0 & 0 & v(m-Y_{\dot{v}}) & u(X_{\dot{u}}-m) & 0 \\ 0 & w(m-Z_{\dot{w}}) & v(m+Y_{\dot{v}}) & 0 & r(J_z-N_{\dot{r}}) & q(M_{\dot{q}}-J_y) \\ w(Z_{\dot{w}}-m) & 0 & u(m-X_{\dot{u}}) & r(N_{\dot{r}}-J_z) & 0 & p(J_x+K_{\dot{p}}) \\ v(m-Y_{\dot{v}}) & u(m+X_{\dot{u}}) & 0 & q(J_y-M_{\dot{q}}) & p(J_x+K_{\dot{p}}) & 0 \end{bmatrix} \qquad (6)$$

The drag produced by the RoboSalmon as it moves is modeled using the summation of two components, one is the drag for the vehicle hull and the other is the drag due to the caudal fin. Both drag components use the standard rigid body drag calculated using Equation (7) [Hoerner, S. F., 1965].

$$D=-0.5\rho C_D A|u|u \qquad (7)$$

Where D is the rigid body drag (N), ρ is the water density (kgm^{-3}), A is the frontal area (m^2) and u is the velocity (ms^{-1}). For the purposes of calculating the drag coefficient C_D for the body it is assumed to be a streamlined cylinder. Drag in the x-y plane is also assumed to be that of an ellipse shaped body and an additional wedge shaped term to represent the caudal fin. Within this equation it is the area (A) that varies depending on the fin pitch.

2.3 Vehicle Kinematics

The vehicle velocities and accelerations generated by the dynamics of the model are calculated with respect to a reference frame attached to the body. To translate such body fixed velocities to velocities in the inertially fixed Earth frame a transformation is required. Two transformation matricies are used, one for the linear velocities (u,v,w) shown in Equation (8) [Fossen, T.I., 1994] and one for the angular velocities (p,q,r) shown in Equation (9) [Fossen, T.I., 2002].

$$\dot{\eta}_1=J_1(\eta_2)\upsilon_1 \qquad (8)$$

$$\dot{\eta}_2=J_2(\eta_2)\upsilon_2 \qquad (9)$$

where υ_1 is the linear velocity components of υ and υ_2 is the angular velocity components of υ, η_1 and η_2 are the linear and angular velocities in the earth fixed frame respectively and J_1 and J_2 are the transformation matrices.

3. ROBOSALMON PROPELLER MODEL

The model for the propeller driven RoboSalmon is developed using the same methodology, assumptions and standard marine equations used for the tendon drive system. Like the RoboSalmon tendon drive model, the

propeller driven vehicle model is divided into three sections; Propulsion system modeling, Vehicle dynamics and the vehicle kinematics.

3.1 Propulsion System Modeling

The propeller is driven by a MFA Comodrills RE540/1 DC Motor with a 11:1 reduction gearbox [MFA Comodrills, 2008]. The rudder is actuated by a Hitec HS-311 Analog Servo motor [Hitec RCD, 2007]. The propeller used for the system is a brass, 3 blade, 40mm in diameter prop used for model marine applications.

The thrust produced by the propeller has been estimated experimentally and is a function of the propeller rotational speed. This thrust estimate is used for the thrust generated by the propeller in the model.

The rudder and propeller model are constrained to what is possible from the hardware which is under development. Input voltage to the DC motor driving the propeller is limited to 12V, which is the maximum battery voltage available. The rudder defection is limited to ±20 degrees

3.2 Vehicle Dynamics

The dynamics of the propeller driven vehicle are modeled using the same standard dynamic equations as the tendon drive RoboSalmon shown in Equation (3). The main difference between the dynamics of the tendon drive and the propeller driven vehicle is the way drag is calculated. As the propeller vehicle has a rigid hull there is no additional term for the drag of the moving tail and caudal fin.

Added Mass is calculated using the standard equations for a prolate ellipsoid [Fossen, T.I., 1994].

4. SIMULATION RESULTS

The RoboSalmon vehicle models are converted into state space form and simulated in the MATLAB environment. The simulation is a multirate simulation with the motor dynamics and the vehicle dynamics being evaluated at different integration step sizes. This was done to reduce the processing time for each simulation run. Other vehicle models in different application areas have benefited using different simulation rates for the motor dynamics and vehicle dynamics [Worrall, K.J. and McGookin, E.W., 2006].

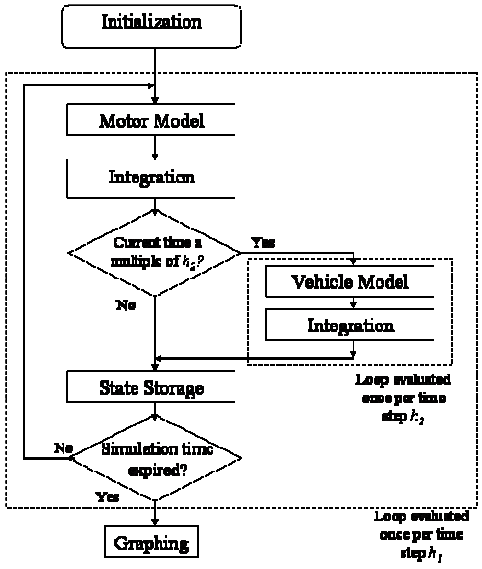

Figure 7. Flow of multirate simulation used for vehicle models

The vehicle models have been evaluated through a number simulations. Simulation results for three aspects of the models are shown below, Forward Propulsion, Turning Circle and Zig-Zag Maneuver.

4.1 Forward Propulsion

Shown in Figure 7 is the simulation results for forward propulsion at the maximum allowable input parameters, which are determined by the hardware currently under development. For the Tendon drive system this is a tail beat frequency of 1Hz and for the propeller system it is an applied voltage of 12V to the DC motor driving the propeller.

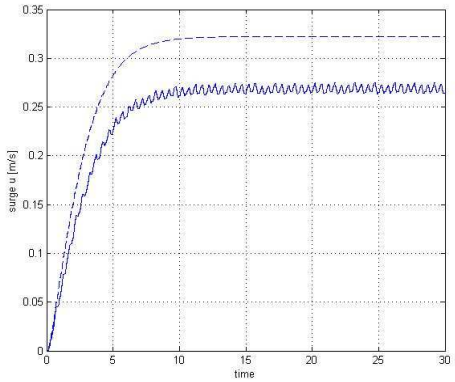

Figure 8. Simulated Maximum Surge velocity for Tendon drive System (solid line) and propeller system (dashed line).

This shows that the maximum obtainable surge velocity from the propeller based system is greater than the tendon drive system. It also indicates that the maximum surge velocity is most likely less than that of real Salmon [Videler, J. J., 1993]. Preliminary results obtained from the initial prototype indicate that the simulated surge velocities are comparable with the experimental surge velocities.

4.2 Turning Circle

Shown in Figure (8) is the simulated turning circle for both types of propulsion system estimated.

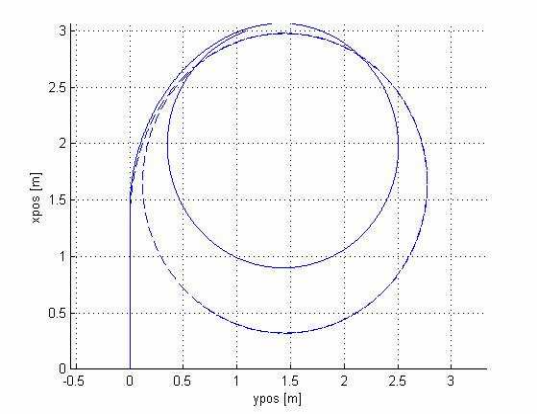

Figure 9. Simulated turning circle for tendon drive system (solid line) and propeller/rudder system (dashed line).

The simulation is carried out with the tail centerline and rudder angle at their maximum values and the tail beat frequency at 1Hz and the 12V propeller motor voltage. This simulation shows that the tendon drive system is capable of achieving a smaller steady turning radius of 1.08m compared with a steady turning radius of 1.33m for the prop/rudder system.

4.3 Zig-Zag Maneuver

Shown in Figure 9 is the simulated response to both vehicles to a zig-zag maneuver.

The zig-zag maneuver is generated by setting the rudder/tail centerline to its maximum value until a yaw angle of 20 degrees is reached. Once 20 degree yaw angle is reached the rudder andgle is reversed until a -20 degree yaw angle is reached.

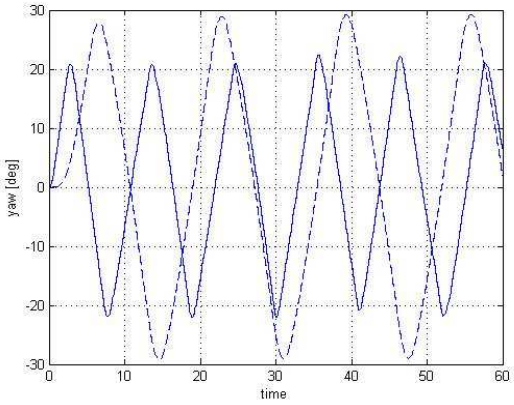

Figure 10. 20-20 Zig-Zag maneuver for tendon-drive system (solid line) and propeller/rudder system (dashed line)

Figure 9 shows that both vehicles are capable of completing the maneuver but the tendon drive system can complete the change in direction faster than the propeller/rudder system. Also, there is a larger percentage overshoot in the propeller/rudder system with a maximum overshoot of around 40% overshoot compared to an 11% overshoot for the tendon drive system.

5. CONCLUSIONS

This paper has presented a simple mathematical model of a biomimetic fish-like vehicle called the RoboSalmon which utilizes a tendon drive propulsion system. Development of the model is described. The development of the models provides a framework that allows for different types of actuation schemes for biomimetic propulsion systems to be evaluated. Simulation results of the tendon drive vehicle and the propeller drive vehicle with their current set up show that the propeller drive system allows for a greater maximum surge velocity when both vehicles inputs are at their maximum allowable limit. Simulation of turning circle and of zig-zag maneuver indicate that the tendon drive system may provide improved maneuverability with a smaller steady turning radius and less overshoot during course changes. For these reasons and the other potential benefits of biomimetic propulsion systems discussed earlier, use of a fish-like propulsion system may be preferred in certain applications.

The development of these simple mathematical models provides a framework for evaluating the performance of different types of actuation systems for biomimetic propulsion systems.

References

Behnke, S., Schreiber, M., 2006, "Digital Position Control of Analog Servos", Proceedings of the IEEE-RAS International Conference on Humanoid Robotics, Genoa, Italy, pp 56-61

Burcher, R. and Rydill, L., 1994, "Concepts in Submarine Design", Cambridge Ocean Technology Series 2, Cambridge University Press

Craig, J.J., 1989, Introduction to Robotics, Addison-Wesley

Fossen, T.I., 1994, Guidance and Control of Ocean Vehicles, John Wiley & Sons Ltd

Fossen, T.I., 2002, Marine Control Systems, Marine Cybernetics.

Franklin, G., Powell J., Emama-Naeini, A, 1991, Feedback Control of Dynamic Systems 2nd Edition, Addison-Wesley Publishing Company

Hitec RCD, 2007, Company Website, http://www.hitecrcd.com, consulted May 2008

Hoerner, S. F., 1965, Fluid Dynamic Drag: Practical Information on Aerodynamic drag and Hydrodynamic Resistance, Published by the Author, Brick Town, New Jersey.

Lighthill, M.J., 1960, "Note on the swimming of Slender Fish", J. Fluid Mech., 9, pp. 305–317

Liu, J., Dukes, I. & Hu, H., 2005, "Novel Mechatronics Design for a Robotic Fish", IEEE/RSJ International Conference on Intelligent Robots and Systems (IROS), Edmonton, Canada, pp2077-2082

MFA Comodrills, 2008, Company Website http://www.mfacomodrills.com, consulted April 2008

Niku, S.B, 2001, Introduction to Robotics - Analysis, Systems, Applications, Prentice Hall, pp 67-76

Sfakiotakis, M., Lane, D.M. & Davies, J.B.C, 1999, "Review of Fish Swimming Modes for Aquatic Locomotion", IEEE Journal of Oceanic Engineering, Vol. 24, No. 2, April 1999

Triantafyllou, M.S. & Triantafyllou, G.S., 1995, "An Efficient Swimming Machine", Scientific America.

Videler, J. J., 1993, Fish Swimming, Fish and Fisheries Series 10, Chapman & Hall

Wardle, C.S., Reid, A., 1975, "The Application of Large Amplitude Elongated Body Theory to Measure Swimming Power in Fish", Fisheries Mathematics, Edited by J.H. Steele, Proceedings of Conference Institute of Mathematics and its Applications, November 24-26, Aberdeen

Watts, C., McGookin, E., Macauley, M., June 2007, "Modelling and Control of a Biomimetic Underwater Vehicle with a Tendon Drive Propulsion System", IEEE/OES Oceans 2007 Europe, Aberdeen

Wernli, R.L., 2002, "AUVs-a technology whose time has come", Proceedings of the 2002 International Symposium on Underwater Technology, 2002, pp309- 314

Wolfgang, M.J., Anderson, J.M., Grosenbaugh, M.A., Yue, D.K.P., Triantafyllou, M.S., 1999, "Near-body Flow Dynamics in Swimming Fish", The Journal of Experimental Biology 202, p 2303-2327

Worrall, K.J. and McGookin, E.W., 2006, "A Mathematical Model of a Lego Differential Drive Robot ", 6th UKACC Control Conference, Glasgow, UK, 30th August–1st September.

Young, J.Z., 1962, The Life of Vertebrates, Second Edition, Oxford University Press, pp 204-206

Yu, Junzhi, Shuo Wang and Min Tan, 2005 , "A simplified propulsive model of bio-mimetic robot fish and its realization", Robotica Vol 23, pp. 101–107.